PHYSICAL REVIEW B VOLUME 52, NUMBER 3 15 JULY 1995-I

Helium-atom-scattering study of the dispersion curves of step-localized phonons on Cu(211) and Cu(511)

G. Witte, J. Braun, A. Lock,* and J.P. Toennies
Max-Planck-Institut für Strömungsforschung, Bunsenstraße 10, D-37073 Göttingen, Germany
(Received 8 February 1995)

The surface phonon dispersion curves of two different regularly stepped vicinal copper surfaces have been measured using high resolution inelastic helium-atom scattering. The Cu(211) and Cu(511) surfaces were chosen since they have comparable step distances but different terrace orientations (111) and (100), respectively. The Rayleigh mode was measured over the entire Brillouin zone along azimuths parallel and perpendicular to the step edge directions. For both surfaces backfolding of the Rayleigh mode was observed along the direction perpendicular to the step edges, while parallel to the step edges, a step localized mode with optical character and a weak dispersion were also found. For the Cu(511) surface, an additional longitudinal mode and an energy gap for the Rayleigh mode at the zone boundary could be identifed, whereas on Cu(211), an additional horizontal mode could be identified. The low zone boundary energy observed for the latter mode can be related to the relaxation of the step atoms. The experimental data can be well explained by theoretical slab calculations in the framework of a single force constant model.

I. INTRODUCTION

Structural defects on metal surfaces are presently considered to be sites of special chemical activity (active sites) and are thus of key importance in many chemical surface reactions.[1] Regularly stepped surfaces appear to be good model systems for real surfaces with their large number of intrinsic defects such as adatoms, steps, and vacancies. The structure of stepped surfaces has been extensively studied since they show a variety of specific properties. For example, the roughening transition,[2,3] facetting,[4,5] and the nucleation in crystal growth[6,7] have been investigated using diffraction experiments with He-atom beams (HAS) or electrons [low energy electron diffraction (LEED)]. More recently due to the availability of the scanning tunneling microscope (STM), structural features of single steps can be monitored and quantities like step-step interaction and kink formation energies could be evaluated.[8–11] The lattice dynamics is also expected to be modified for stepped surfaces compared to the low index flat surfaces, as the presence of step edges reduces the inherent surface symmetry and the new surface unit cell contains a larger number of atoms. Therefore, the existence of additional modes, especially step localized modes and backfolded optical modes, is anticipated. These are expected to be sensitive to the structural and electronic relaxation at the step edge.

Although surface phonons on low Miller-index surfaces have been extensively studied experimentally,[12] so far only a few mostly theoretical studies of stepped surfaces have been reported. Since traditional lattice dynamical calculations require large dynamical matrices for stepped surfaces the calculations were only performed at high symmetry points of the Brillouin zone (BZ).[13–15] The few EELS measurements were all made at the origin of the BZ.[16,17] He atom scattering (HAS) has a greater resolution than the electron energy loss spectroscopy (EELS) (Ref. 18) and is more sensitive to the step edges[4] and this technique was used in the first measurements of surface phonon dispersion curves for the stepped metal Al(221) surface.[19] The great sensitivity of HAS to disorder when compared with EELS limits the admissible defect concentration and this hampered the interpretation of these results.

In this paper, we report on a high resolution HAS investigation of the surface phonons of the Cu(211) and Cu(511) surfaces. Copper was chosen in the present study since it does not roughen during preparation of well ordered surfaces. The very good order was indicated by sharp diffraction peaks so that it was possible to measure a complete set of dispersion curves throughout the entire BZ for both symmetry directions parallel and perpendicular to the step edge direction. These copper surfaces have the further advantage that the phonons on the corresponding terraces have recently been extensively investigated, both experimentally and theoretically.[20,21] The present experimental dispersion curves were analyzed with realistic lattice dynamical calculations. These calculations also yield valuable information for optimization of the experimental conditions.

The paper is organized in the following way. First, we provide a description of the geometry of the investigated stepped surfaces in Sec. II. The experimental setup and the characterization of surface structure are outlined in Sec. III. Time-of-flight results and phonon dispersion curves are presented in Sec. IV. In Sec. V, results of the lattice dynamical calculations are presented and discussed. The paper closes with a discussion and suggestions for future research in Sec. VI.

II. GEOMETRY

Assuming only monatomic steps and close packed (i.e., nonkinked) step edges, all vicinal fcc surfaces can be di-

TABLE I. Classification of stepped surfaces with close packed step edges (Refs. 14 and 15).

Class	Miller index ($n \geq 2$)	Terrace face	Step face	Step edge	BZ type	Example
A	$(n+2,n,n)$,n even	(111)	(100)	$[01\bar{1}]$	P rect.	(211)
	$(n+2,n,n)$,n odd	(111)	(100)	$[01\bar{1}]$	C rect.	(533)
B	$(2n-1,1,1)$	(100)	(111)	$[0\bar{1}1]$	C rect.	(511)
C	$(n,n,n-2)$,n even	(111)	(111)	$[\bar{1}10]$	P rect.	(221)
	$(n,n,n-2)$,n odd	(111)	(111)	$[\bar{1}10]$	C rect.	(331)

vided into three classes designated A, B, and C (see Table I).[14,15] In the present experiment we have investigated stepped surfaces, which are representative of classes A and B. The previously studied Al(221) surface[19] belongs to class C. As shown in Fig. 1, both the Cu(511) and Cu(211) surfaces consist of terraces (100) and (111), respectively, each containing three atom rows separated by a monoatomic step. The angles α formed between the terrace plane and the macroscopic surface (i.e., the nominal Miller-indexed surface plane) are 15.8° and 19.5° for the Cu(511) and Cu(211) surfaces, respectively. While both surfaces have nearly the same step separation d, they have complementary terrace and step face orientations. Both surface unit cells contain three atoms with one step or step edge atom (atom 1 in Fig. 1) and two terrace atoms. Due to the different surface symmetry, the corresponding surface Brillouin zones are of P-rectangular type for Cu(211) and C-rectangular type for Cu(511),[14] respectively. In the calculations, we use a coordinate system with the z-axis perpendicular to the macroscopic surface. The x axis is chosen to be along the step edge and the y-axis perpendicular to the step edge.

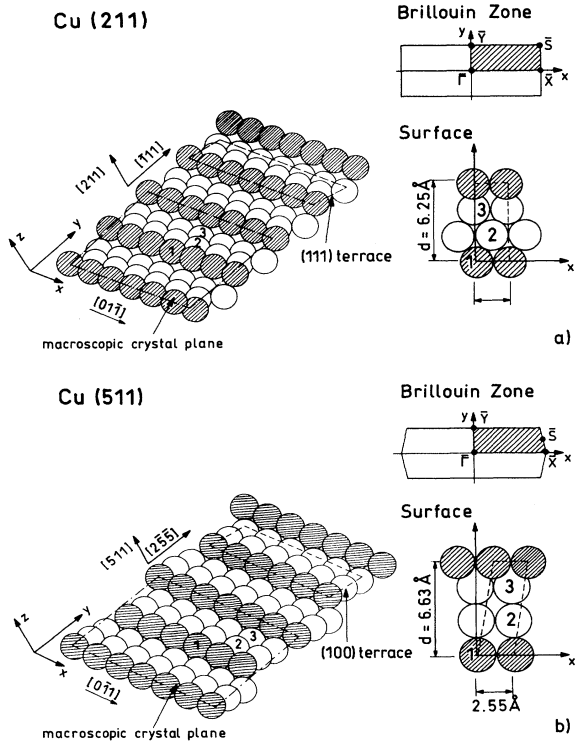

FIG. 1. Geometries of the Cu(211) and Cu(511) surfaces. The perspective ball models show the composition and the important directions of the surfaces. The hatched circles denote step edge atoms. The surface unit cells are shown from above on the right. Both surface unit cells contain three atoms. Also shown are the corresponding surface Brillouin zones.

III. EXPERIMENTAL SETUP AND SAMPLE PREPARATION

In the He scattering apparatus, which is described in detail elsewhere,[4] a well collimated nearly monoenergetic helium-atom beam is directed at the surface. The scattered atoms are detected at a fixed total scattering angle of 90.5°, with respect to the incident beam, while the angle of incidence and scattering can be varied by rotating the crystal with a resolution of 0.05°. The overall angular resolution of the apparatus is about 0.2°. The energy of the He-atoms beam can be varied between 10 and 120 meV ($k_i = 4.4 - 15.2$ Å^{-1}), with a velocity distribution of $\Delta v/v = 0.75\%$, by changing the source temperature from 35 to 500 K, respectively. The time-of-flight (TOF) analysis of the scattered atoms allows the observation of discrete (one-phonon) inelastic scattering processes with a typical overall energy resolution of 0.4 meV. Signals over a range of about 5×10^6 can be handled without any saturation effects.

The copper single crystals with (511) and (211) surfaces, which had been polished within ±0.1° of the desired orientation, were prepared in UHV (base pressure 1×10^{-10} mbar) by repeated cycles of Ar^+ ion bombardment (800 eV, 30 min) and subsequent annealing to 800 K until no traces of sulfur, carbon, and oxygen were found in the recorded x-ray photoemission spectroscopy spectra within the detection limit of 0.5% of a monolayer.

After sample preparation, the surface structure was characterized by helium-atom diffraction, which was measured by rotating the crystal. The parallel momentum transfer for elastic scattering is given by $\Delta K_{\parallel} = k_i(\sin\theta_i - \sin\theta_f)$, where θ_i is the incident angle and $\theta_f = 90.5° - \sin\theta_i$. In order to minimize multiphonon excitation and inelastic broadening of the diffraction peaks, the measurements were performed at low crystal temperatures of 100 – 150 K. Figure 2(a) shows typical HAS angular distributions taken along the azimuth direction uphill and perpendicular to the step edges. Many intense diffraction peaks up to the ± sixth order are observed. From the positions of the diffraction peaks in the angular distributions, taken over a wide range of initial He-atom wave vectors k_i between 4.6

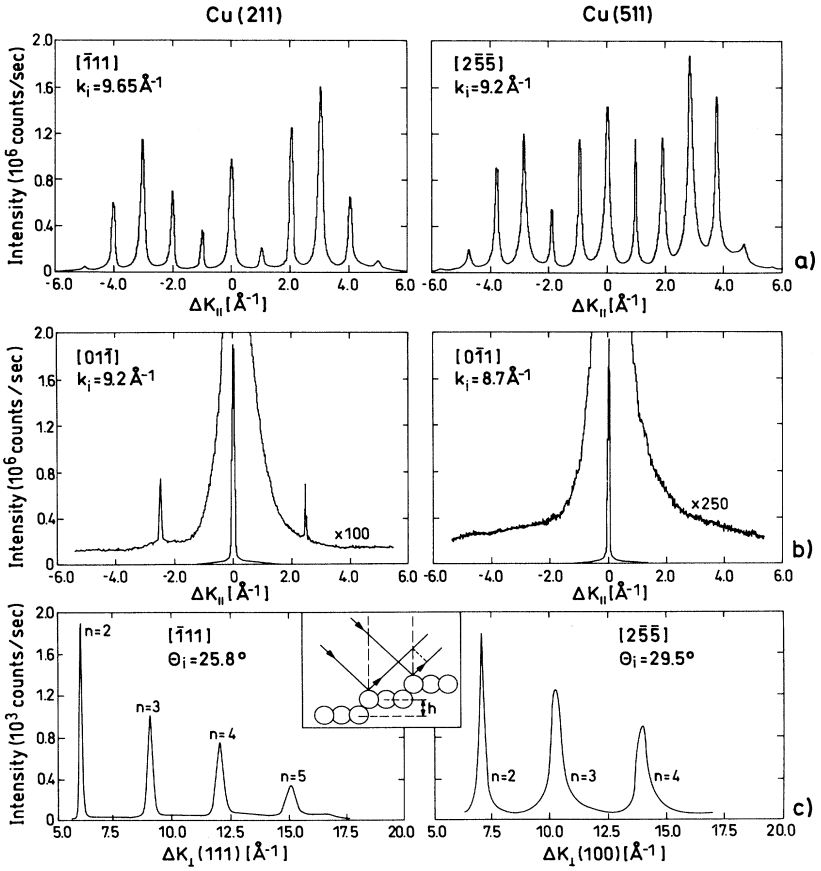

FIG. 2. Comparison of different HAS angular distributions for Cu(511) and (211). (a) Angular distributions perpendicular to the steps. (b) Angular distributions along the step edge direction. (c) Intensity of the terrace specular peak for a controlled variation of the incident He-beam energy ("drift spectrum") as a function of the perpendicular momentum transfer. The observed maxima correspond to in-phase conditions for constructive interference between neighboring terraces separated by the step height h as shown in the inset).

and 14.6 $Å^{-1}$, the average step separation d was determined to be 6.65 (±0.08) Å and 6.28 (±0.08) Å for the Cu(511) and Cu(211) surfaces, respectively. The separation is in good agreement with the ideal separations of 6.62 Å and 6.25 Å. As discussed previously, HAS exhibits very strongly enhanced form factors for step edge atoms in comparison to the diffraction of low energy electrons.[4] Consequently, the observed step edge scattering is relatively intense and this enables a very accurate determination of step edge distributions.[22] The presence of defects will lead to additional interference and there exist (three dimensional) Bragg conditions, where scattering from all possible steps within the beam coherence length are in phase. Accordingly diffraction peaks observed for an anti-Bragg (AB) condition are broadened and their full width at half maximum (FWHM) is determined by the lateral step ordering. After deconvolution with the beam energy width and the angular resolution from the FWHM of the step diffraction in the AB condition, the surface coherence length perpendicular to the steps is estimated to be about 72 Å and 63 Å for the Cu(511) and Cu(211) surfaces.

For scattering along the step edge direction, no diffraction was obtained for the (511) surface. However, for the Cu(211) surface a weak first order diffraction peak was observed with an intensity of 3×10^{-3}, relative to the specular peak [see Fig. 2(b)]. For the corresponding azimuthal direction on a flat Cu(111) surface, no diffraction has yet been reported.[20] Furthermore, as far as we are aware, no diffraction has ever been found along the rows on the Cu(110) and Cu(113) surfaces.[23] Since the specular peak shows neither a broadening nor a foot, a periodic arrangement of kinks can be excluded as causing this diffraction peak. The enhanced corrugation is probable due to an enhanced corrugation of the surface caused by a redistribution of electron charge away from the step atoms. For both surfaces, an average kink distance of more than 130 Å along the step edges was estimated from the width of the specular peak. Since the diffraction peaks along the direction perpendicular to the step edge are broader, we conclude that the main defects are nonkinked extra steps with terraces, which differ from the ideal terrace width.

Figure 2(c) shows the intensity of the terrace specular peak during a controlled linear variation of the beam source temperature ("drift" spectrum), which leads to a scan over the incident wave vector. The equidistant intensity maxima as a function of the (elastic) momentum exchange perpendicular to the terraces correspond to conditions where atoms are constructively scattered in-phase from neighbouring terraces. Using the relationship for these maxima: $h = n2\pi/\Delta k_z$, step heights h of 1.84 (±0.05) Å, and 2.03 (±0.05) Å are determined in good agreement with the expected values of 1.81 Å and 2.08 Å for the ideal Cu(511) and Cu(211) surfaces, respectively.

The absence of intermediate maxima and the low intensity at the out-of-phase minima indicate the absence

of double and multiple steps and the corresponding large smooth terrace facets. It should be noted that the good agreement of the step height with the ideal spacing of bulk planes does not exclude any step atom relaxation. Since the He atoms are scattered mainly from the step atoms due to their large form factors, a relaxation of the steps, with respect to the terraces, cannot be observed. Most angular distributions were measured for surface temperatures between 130 and 300 K and they revealed no significant temperature dependence. In addition, no indication of roughening was observed in this temperature regime.

The same samples were used in a separate spot profile analysis–LEED experiment.[24] An analysis of the shape of the diffraction spots indicates that about 90% of the terraces have the nominal length. Recent STM measurements on a Cu(211) sample also confirm the excellent order of the surface at low temperatures.[25]

IV. SURFACE PHONON DISPERSION CURVES

The surface phonon dispersion curves were measured for both surfaces along the two symmetry directions, ($\overline{\Gamma X}$) parallel and ($\overline{\Gamma Y}$) perpendicular to the step edges. The TOF spectra were measured for low surface temperatures of between 100 and 140 K in order to suppress the multiphonon background. For the $\overline{\Gamma Y}$ direction the large corrugation causes diffraction mediated scattering processes with large parallel momentum transfer $\Delta K = Q \pm G$ to occur with a large probability. Q is the phonon wave vector and G is a reciprocal lattice vector.

Figure 3(a) illustrates the relationship between the angular distribution and the measured phonon dispersion curves for the Cu(211) surface in an extended Brillouin zone scheme [Fig. 3(b)] measured for the same incident energy. Also shown are two typical TOF spectra and their corresponding scan curves (dash-dotted lines in Fig. 3(b). Compared to the corresponding time-of-flight spectra for the low index terrace surfaces the TOF spectra along the $\overline{\Gamma Y}$ direction are always dominated by a large elastic peak. This is presumably caused mainly by diffuse scattering from defective steps, which are separated by distances differing from the ideal step separation. Since in Fig. 3(b) all the phonon scattering is diffraction mediated, the phonon wave vector resolution is limited by the broadening of the diffraction peak.[26] Moreover, since the inelastic intensity in the TOF spectra is proportional to the corresponding (elastic) diffraction intensity,[27] which is distributed over several peaks, the inelastic intensity in the TOF spectra is greatly reduced especially at the AB condition compared to a low index surface. Since the phonon intensity is smaller than for low indexed surfaces, most of the TOF measurements took between 30 and 60 min for each angle. A further problem arises from spurious peaks in the TOF spectra. These so-called "deceptons" are caused by elastic diffraction from the weak, energetically broad Maxwellian background in the incident beam.[18] However, these features (D) can be easily identified, since they lie on a characteristic curve shown in Fig. 3(b) as dotted lines. The corresponding spectra perpendicular to the step edges for the Cu(511) surface are shown in Fig. 4(a).

The TOF spectra for the $\overline{\Gamma X}$ direction (parallel to the step edges) for both surfaces are shown in Figs. 4(b,c). For the Cu(211) surface, additional measurements were performed in an out-of-plane geometry. This was achieved by tilting the crystal to the second order diffraction peak in $\overline{\Gamma Y}$ direction, and then TOF measurements were taken parallel to $\overline{\Gamma X}$. An example is shown in the trum of Fig. 4(c). For this scattering geometry, a new low energy phonon mode (labeled T) is confirmed, which is only visible as a shoulder for in-plane scattering, indicating that this mode has a large horizontal polarization component.

The entire set of phonon dispersion curves in the first BZ for both surfaces are presented in Fig. 5. For the Cu(211) surface [Fig. 5(a)] the Rayleigh mode has a $\overline{Y}$

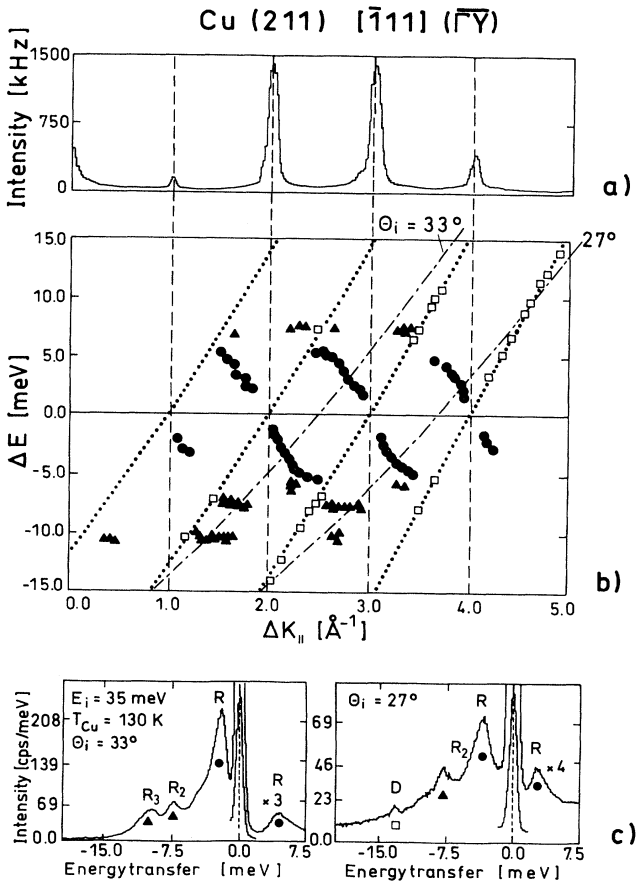

FIG. 3. All phonon inlastic peaks measured with an incident energy of 35 meV along the $\overline{\Gamma Y}$ direction for the Cu(211) surface are plotted in an extended zone scheme representation. (a) Angular distribution recorded for the same incident energy. (b) Dispersion curves in the extended zone diagram show many of the phonon branches that correspond to diffraction mediated processes. These processes occur only if the corresponding diffraction peaks are intense, as shown in (a). (c) Two typically TOF spectra are shown together with their corresponding scan curves [dashed-dotted line in (b)]. Sometimes virtual "decepton" peaks appear in the TOF spectra, which are located on characterictic curves [dotted lines in (b)].

point zone boundary energy of 5.5 meV. Two additional modes or resonances ($R2$ and $R3$) at around 7.6 and 10.5 meV were also observed near $\overline{Y}$ [see Figs. 3(b,c)]. Along the step row direction ($\overline{\Gamma X}$), the Rayleigh mode (R) and the horizontal mode (T) could be measured nearly out to the zone boundary with an extrapolated zone boundary energy of 14 ($\pm$ 1) meV for the Rayleigh mode. For wave vectors at 0.8 $\overline{\Gamma X}$, the horizontal mode energy is 10.3 meV and lies about 4 meV below the Rayleigh mode. The flat step mode (E) starts at 10.9 meV at the $\overline{\Gamma}$ point and lies above the Rayleigh mode. While this mode is very intense for small wave vectors the intensity decreases more rapidly with increasing wave vectors than the Rayleigh mode. In addition, at about 0.5 $\overline{\Gamma Y}$, some very weak peaks (labeled B in Fig. 5) with energies of about 16 meV were observed, which can be attributed to a bulk resonance.

On the Cu(511) surface, three modes were observed in the $\overline{\Gamma Y}$ direction. The lowest energy mode (R) has an energy of 6.3 meV at the $\overline{Y}$ point, where it is folded back leading to an optical branch (O) with an energy gap of about 0.8 meV at $\overline{Y}$. The high energy optical branch (O) of this mode had only very weak intensity [see Fig. 4(a)]. In addition there is a third intermediate mode (L), which crosses the backfolded branch at 2/3 $\overline{\Gamma Y}$. These higher energy modes are in fact resonances. They are difficult to detect with HAS not only because of their higher energy and their optical character, but also because they overlap with the bulk bands and, therefore, their amplitude at the surface is greatly reduced.

Also, along the $\overline{\Gamma X}$ direction, a Rayleigh mode (R) and a step mode (E) are found. Because of weak phonon peak intensities with wave vectors close to the zone boundary, the $\overline{X}$ point Rayleigh mode energy can only be determined with some uncertainty to be 13.5 ($\pm$ 1) meV. At the $\overline{\Gamma}$ point, the step mode (E) has an energy of 11.5 meV and goes over to the backfolded branch (O) in the $\overline{\Gamma Y}$ direction. This nearly flat mode lies above the Rayleigh

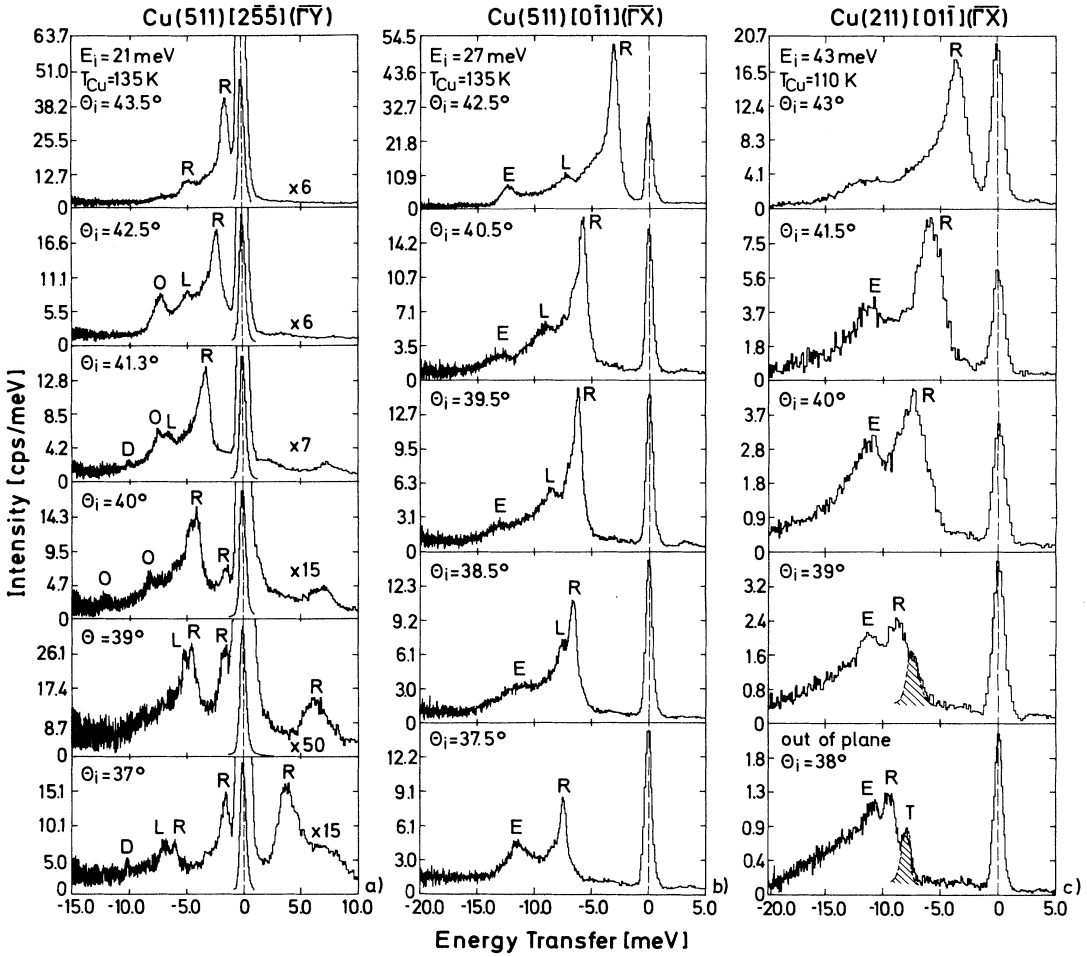

FIG. 4. (a) Series of TOF spectra converted into an energy transfer scale along the $\overline{\Gamma Y}$ direction for the Cu(511) surface. The measurements were taken at a surface temperature of 135 K, with an incident energy of 21 meV. Although the spectra are dominated by a strong diffuse elastic peak, different inelastic phonon loss peaks are found (labeled R, L, and O). (b) TOF spectra recorded with an energy of 27 meV along the $\overline{\Gamma X}$ direction of the Cu(511) surface. For this azimuth three modes were found (labeled R, E, and L). (c) TOF spectra for the $\overline{\Gamma X}$ direction of the Cu(211) surface taken with an incident energy of 43 meV. Note that in the last spectrum in (c), which was measured for an out-of-plane condition, the hatched peak (T) is enhanced, which for the in-plane geometry appears only as an unresolved shoulder.

TABLE II. Experimental zone boundary phonon energies (in meV) for the Cu(211) and Cu(511) surfaces.

	$\overline{Y}$				$\overline{\Gamma}$		$\overline{X}$	
	R	R_2	R_3	O/L	E	T	R	E
Cu(211)	5.5 ±0.2	7.6 ±0.4	10.5±0.3		10.9 ±0.2	11.1 ±1	14±1	14 ±1
Cu(511)	6.3±0.3			7.1±0.4	11.5±0.2		13.5±1	16±1

mode and has an extrapolated zone boundary energy of 16 (± 1) meV. Beside these modes, some weak phonon loss peaks were observed, which are attributed to a longitudinal resonance (L). This mode has a large slope at the $\overline{\Gamma}$ point and crosses the edge mode at 0.4 $\overline{\Gamma X}$. Table II lists the zone boundary energies of all observed modes for both surfaces.

Finally, it should be noted that these results on stepped surfaces cannot be compared directly with the surface phonons measured on the corresponding low index surface planes. Because of the large scattering cross sections, large amplitudes of the step edge atoms HAS in the former case is sensitive mainly to the phonon modes at the step edges. However, the edge atoms have a reduced coordination number and, therefore, exhibit entirely different dispersion curves than the corresponding terraces. Thus, the two sets of measurements complement each other nicely.

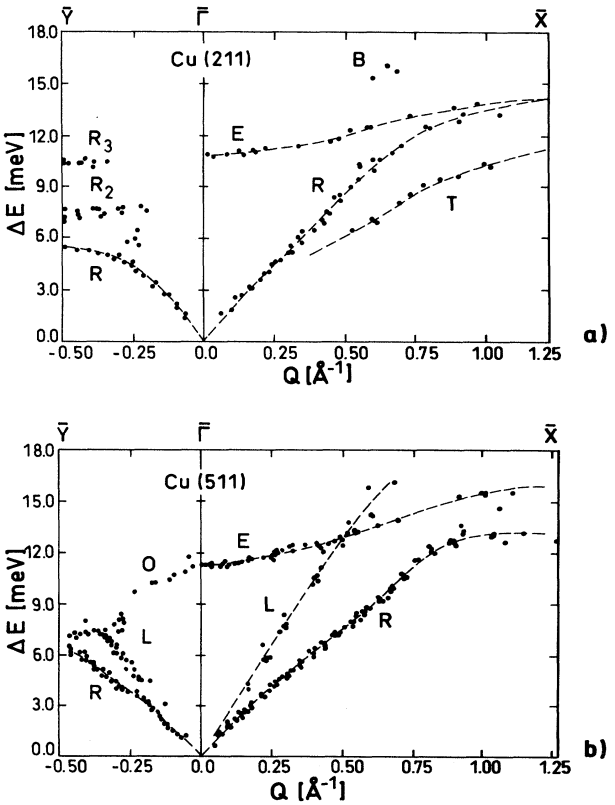

FIG. 5. The experimentally determined surface phonon dispersion curve for the Cu(211) (a) and Cu(511) (b) surfaces. Along the $\overline{\Gamma Y}$ direction, all the measured phonon peaks have been folded back into the first Brillouin zone.

V. LATTICE DYNAMICAL SLAB CALCULATIONS

In order to gain detailed insight into the displacement patterns and the polarization of the observed modes, theoretical simulations are necessary. Previous calculations of the phonons of these surfaces were restricted to high symmetry points,[14] including the backfolding of surface modes.[13] Only recently, calculations for the whole dispersion curves for vicinal surfaces have become available.[15,19] Using the slab method originally proposed by Allen *et al.*[28] lattice dynamical calculations were carried out for large slabs with (511) and (211) surface terminations. In our approach, a computer algebra program was utilized to generate the atomic positions of all the atoms in the slab unit cell and to set up the elements of the dynamical matrix for a crystal slab with surfaces of given Miller indices.[29] For a first order description of the step phonons arising from the specific surface geometry, only a single radial force constant for the nearest neighbor interactions was considered. The force constant used $\beta = 28$ N/m (Ref. 30) provides a remarkably good fit of the bulk dispersion curves[20,31] without any further fit parameters. Although a refined calculation of the Cu(100) and Cu(111) surface phonons, especially in order to understand HAS TOF intensities, requires the consideration of the electronic degrees of freedom (for example within the pseudocharge model[20]), this simple force constant model is also able to describe the surface phonon dispersion curves in a first approximation. Thus, since our main concern is to assess the effect of the steps on the dynamics and, moreover, since at this stage an extensive fit of inelastic intensities does not appear to be justified, the simple model was used here. In contrast to the flat surfaces, both stepped copper surfaces contain three surface atoms within the surface unit cell with different coordination. Since no detailed information about the relaxation and the local force field for the different surface atoms on the stepped copper surfaces are available, we have also neglected structural relaxation. To simulate the relaxation of the step edge atoms, a softening of the force constants is introduced later on.

In order to avoid artifacts due to an interaction of the two surfaces of the slab, we have performed the numerical calculations for a slab infinitely extended in the x and y directions, having a thickness of 216 atomic layers. This unusually large number of layers was required because of the large size of the unit cell. Figure 6 shows the calculated surface phonon dispersion curves for both stepped copper surfaces along the directions perpendicular ($\overline{\Gamma Y}$) and parallel ($\overline{\Gamma X}$) to the step edges. The character of the phonon modes is derived from an analysis of the corre-

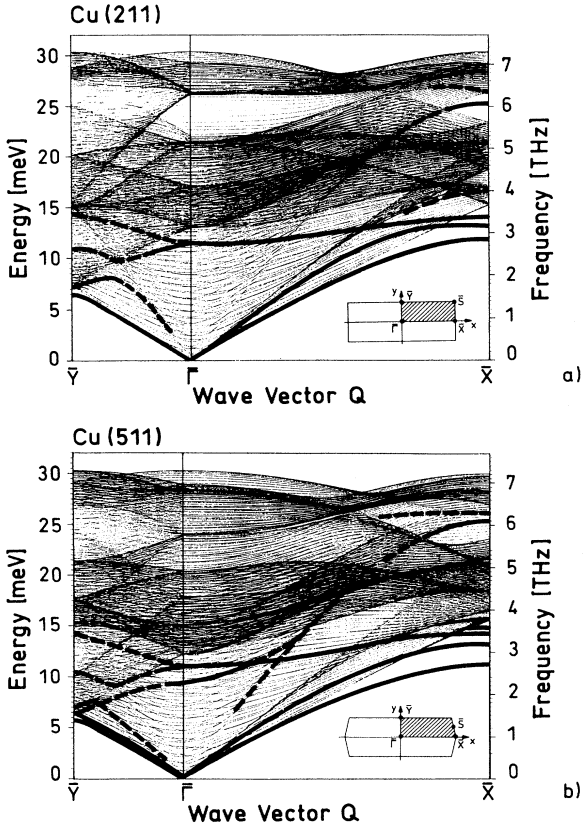

FIG. 6. Calculated phonon dispersion curves for both high symmetry directions for both vicinal copper surfaces. The calculations were performed for a slab with 216 layer with a single nearest neighbor radial force constant without any relaxation. The bold lines show the surface phonon modes, which could be identified from their polarization amplitudes.

sponding polarization vectors and the vibrational density of states, which are presented in Fig. 7 for both surfaces.

A. Surface modes for Cu(211)

Examination of Fig. 7(a) reveals that the lowest energy mode parallel to the step edges ($\overline{\Gamma X}$ direction) is a mainly shear horizontal polarized (T) mode (i.e., polarized along y direction of Fig. 1), with an energy of 11.7 meV at the $\overline{X}$ point. In contrast, the saggital polarized Rayleigh mode (R) is located mainly within the transversal bulk band and has a $\overline{X}$-point zone boundary energy of 13.3 meV. Close to the $\overline{X}$ point, an additional saggital polarized mode appears at 16.5 meV, which peels off from the transverse bulk band and is localized within the third layer. At about 18.1 meV a weak transverse resonance was also found. A further z-polarized mode with a nearly flat dispersion curve, with an energy of 11.4 meV at the $\overline{\Gamma}$ point, which crosses through the bulk bands until it reaches the zone boundary at 14.1 meV, is identified as a step-localized mode. Close to the $\overline{X}$ point, a longitudinal mode (L) peels off from the longitudinal bulk band and appears as a step-localized longitudinal surface mode within the bulk band gap at 25.4 meV. In addition, two further longitudinal resonances with energies of 26.6 and 27.1 meV are found near the zone boundary with maximum displacement in the second and third layer, respectively.

Perpendicular to the steps along the $\overline{\Gamma Y}$ direction, the mode structure is even more complicated. Since the Brillouin zone is so short along this direction ($\overline{\Gamma Y} \leq 0.5$ Å^{-1}), only long wavelength (acoustic) phonon modes with a corresponding large penetration depth are possible. In addition backfolded phonon branches cross (many) bulk bands or surface modes[32] and surface resonances appear. Consequently, many of the modes are localized in several layers or form phonon bands with a considerable width in energy. This behavior is particularly prevalent for the longitudinal and transverse polarized modes and, consequently, only their lowest energy modes could be identified. Since along this direction HAS is mostly sensitive to the displacement of the edge atoms, only the corresponding vibrational density of states are shown for the edge atoms [see Fig. 7(c)].

The lowest energy mode along $\overline{\Gamma Y}$ is a transverse polarized mode with a $\overline{Y}$-point energy of 6.4 meV. The Rayleigh mode has a zone boundary energy of 6.6 meV and forms a small energy gap of 0.4 meV with the backfolded branch. At about 0.5 $\overline{\Gamma Y}$, an avoided crossing of this backfolded branch with a longitudinal bulk band resonance occurs. The folded branch breaks off and hybridizes with the longitudinal mode and thereby loses its z polarization. As a result, the upper part of the longitudinal resonance is mainly z polarized and has an energy of 11 meV at the $\overline{Y}$ point. The continuation of the folded branch has an energy of 11.4 meV at the $\overline{\Gamma}$ point, where it passes over to the step mode. Starting from this point, a further backfolded mode runs to the $\overline{Y}$ point, with a zone boundary energy of 14.5 meV.

B. Surface modes for Cu(511)

Parallel to the step edges ($\overline{\Gamma X}$ direction), several surface modes were found similar to the Cu(211) surface. Again, the lowest energy mode is a horizontal polarized mode, with an energy of 11.4 meV at the $\overline{X}$ point. In comparison to Cu(211), the polarization vectors of this mode has a smaller saggital (z) contribution. The Rayleigh mode, which up to 3/4 $\overline{\Gamma X}$ lies within the horizontal bulk band, has a zone boundary energy of 13.4 meV. The step mode has an energy of 11.2 meV at the zone origin and reaches the $\overline{X}$ point at an energy of 14.5 meV. Very close to the $\overline{X}$ point, a transverse and a saggital polarized mode peel off the bulk band and appear as surface modes at 14.9 meV and 15.6 meV, respectively. Both modes are found to be localized on the terraces (atoms 2 and 3 in Fig. 1). In addition, we note that for the (511) surface, no longitudinal band gap exists at the $\overline{X}$ point. However, a longitudinal mode peels off the longitudinal band with $\overline{X}$ point energy of 25.5 meV and an additional longitudinal resonance exists at about 26.5 meV. The optical longitudinal bulk band edge shows

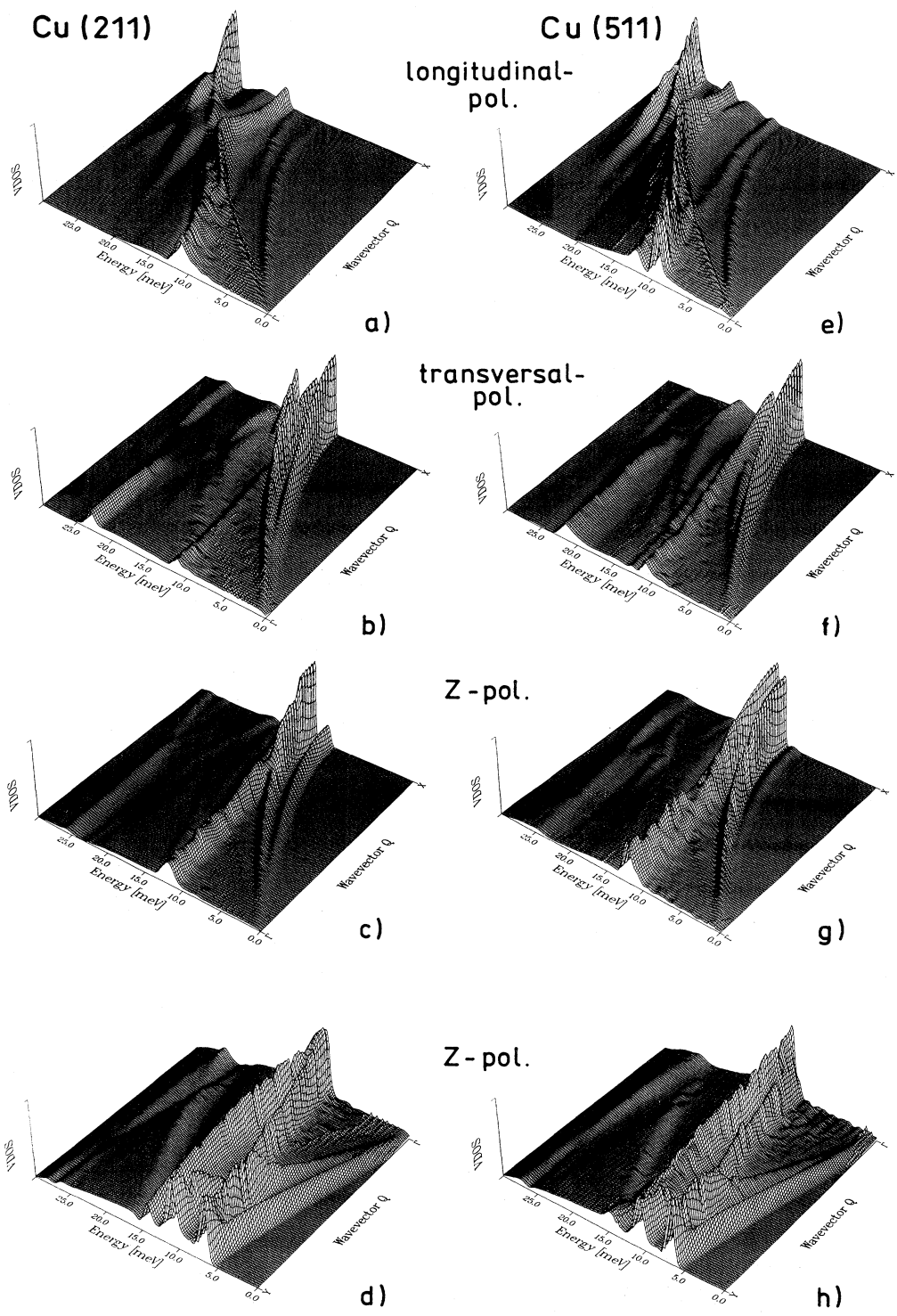

FIG. 7. Calculated vibrational density of states of surface phonons with different polarizations. (a–c) Along the $\overline{\Gamma X}$ direction for the Cu(211) surface. The maximum values are 1.05, 0.78, and 1.28, for the longitudinal, transversal, and z polarization, respectively. (e–g) along the $\overline{\Gamma X}$ direction for the Cu(511) surface. The maximum values are 0.72, 0.97, and 0.91, for the longitudinal, transversal, and z polarization, respectively. (d) and (h) show the density of states for the step atoms for the $\overline{\Gamma Y}$ direction of both surfaces.

a strong density of states similar to the behavior found for the (211) surface. Furthermore, a longitudinal step resonance which does not occur on the Cu(211) surface exists below this band with an energy of 9.6 meV at the $\overline{\Gamma}$ point.

As for the (211) surface, the lowest energy mode along the $\overline{\Gamma Y}$ direction, perpendicular to the steps, is a transverse polarized mode with a $\overline{Y}$ point energy of 5.8 meV. This mode seems to form an energy gap of about 1 meV with the backfolded branch, which acquires longitudinal character and links on to the longitudinal step resonance at the $\overline{Y}$ point. For the Rayleigh mode, a zone boundary energy of 6.5 meV and an energy gap of 0.6 meV with the backfolded branch has been calculated. Again, an avoided crossing arises and the optical Rayleigh-branch splits off at $2/3\ \overline{\Gamma Y}$, while the continuation of the optical branch joins the step mode at the $\overline{Y}$ point. A further backfolded intense mode starts without a gap at the $\overline{\Gamma}$ point and has a $\overline{Y}$ point energy of 14.4 meV.

C. Step modes

To illustrate the nature of the different surface phonon modes runnning along the step edge ($\overline{\Gamma X}$) direction for the Cu(211) surface in more detail, some of the displacement patterns are shown in Fig. 8. For most of the surface modes, a strong localization at the step edges is found. The Rayleigh mode (R) and the step mode (S), which are both saggital polarized, have an orthogonal displacement pattern. At the $\overline{X}$ point, the displacements for the step mode are completely localized at the step edges, while the Rayleigh mode has the largest amplitudes on the terraces. Particularly, the large step atom displacement for the step mode at the $\overline{\Gamma}$ point, which can be attributed to the lower coordination, demonstrate the important role of steps for the lattice dynamics on these surfaces.

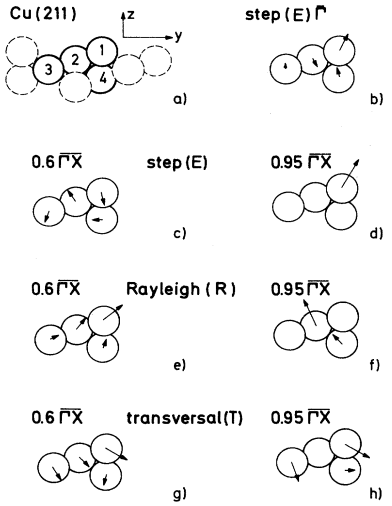

FIG. 8. Atomic displacement patterns for different phonon modes along the $\overline{\Gamma X}$ direction for the Cu(211) surface. (a) Sideview of the surface with the unit cell atoms numbered. (b) Displacement pattern of the step mode at the $\overline{\Gamma}$ point. (c) Displacement pattern of the step mode at $0.6\ \overline{\Gamma X}$, and (d) at $0.95\ \overline{\Gamma X}$. In (e) and (f), the corresponding patterns for the Rayleigh mode and in (g) and (h) for the transversal mode are shown. All displacements are magnified by a factor of 25 relative to the interatomic distances.

D. Relaxation

For the highly corrugated low index metal surfaces, e.g., fcc(110) surfaces and a few vicinal surfaces substantial relaxation of the top layers has been found experimentally and theoretically.[33] There is a general tendency for inward relaxation of the first layer and smaller oscillatory relaxations within the deeper layers. Usually, multilayer relaxations for stepped surfaces are described only in terms of interlayer relaxation, ignoring the geometry of the surface. The only detailed multilayer relaxation calculations available for fcc(211) and (511) surfaces were performed by Jiang, Jonas, and Marcus.[34] Based on a point-ion model, they found a larger step atom relaxation for the Al(211) surface (18% of the nearest neighbor distance) than for the Al(511) (11% of the nearest neighbor distance) surface, as is shown schematically in Fig. 9. Since for Al(110) and Cu(110) a similar relaxation behavior has been found,[33] we feel justified in using those results also as a first approximation for the Cu(211) surface. Since no other detailed information is available on the atomic positions and/or surface stress for these surfaces, we have only carried out some exploratory model calculations to examine the effect of relaxation. To account for the step relaxation, the position of the step atom was relaxed as calculated from Jiang *et al.* and the related interatomic force constants β_{13} and β_{12} (the indices refer to the corresponding atoms as shown in Fig. 9) were changed by $+20\%$ and -20%, respectively. Table III shows a comparison of the high symmetry point phonon energies for the unrelaxed and relaxed surface. The effect of these substantial force constant changes is surprisingly small. The main consequence of the relaxation is a small stiffening of the saggital polarized modes and a softening of the transversal polarized modes, which amounts only to a few percent at the most. The analysis of the

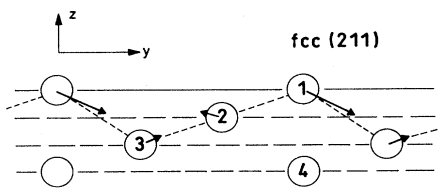

FIG. 9. Schematic diagram of the surface relaxation (Ref. 34). The arrows show the shifts of the atoms, with respect to the ideal surface, and are magnified by a factor of 4 relative to the atomic spacings. The step atom positions and the related interaction forces (1–2, 1–3) are changed in the relaxation calculations described in the text.

TABLE III. Calculated surface phonon energies (in meV) for the ideal and the step relaxed Cu(211) surface.

	at $\overline{Y}$			at $\overline{\Gamma}$			at $\overline{X}$	
Mode	T	R	E	T	R	E
Ideal	6.4	6.6	11.4	11.7	13.3	14.0
Relaxed	6.2	6.7	11.7	11.3	13.2	14.0

corresponding polarization vectors shows no significant changes. We caution that this small effect of relaxation is by no means conclusive and could well be an artifact of the one force constant model. For example, the acoustical step modes at the zone boundary are rather insensitive to the radial force constants and probably more strongly affected by the tangential force constants. Since our model does not contain the latter, it may not be able to properly account for the relaxation effect. A more elaborate force constant model can, on the other hand, not be justified in view of the well known shortcomings of such models[20,21] and their inherent lack of uniqueness.

VI. DISCUSSION

The present experiments and calculations provide the first full set of dispersion curves including the step modes for vicinal surfaces. Up to now the lack of experimental phonon dispersion curves has not made it possible to gauge either the accuracy nor the completeness of previous theoretical studies. These calculations were mainly made for nickel vicinal surfaces for probably two reasons: (1) nickel phonons can be accurately described with a single force constant model and (2) nickel is a well known catalyst. As pointed out in the Introduction, the present comprehensive experiments were performed on copper because of its inertness and the ease with which it is possible to produce structurally nearly perfect surfaces.

In one of the pioneering theoretical investigations Black and Bopp[14] calculated the surface phonon energies at high symmetry points, for a variety of stepped nickel surfaces, using a slab model also with a single nearest neighbor radial force constant β. Since the phonon frequencies are approximately proportional to $\sqrt{\beta/M}$, they can be adapted to other materials using the corresponding values of β/M. Using this transformation, their results were found to be in good agreement ($\pm$ 0.2 meV) with our calculated phonon energies for the zone boundary high symmetry points $\overline{X}$ and $\overline{Y}$ on the Cu(211) surface and for $\overline{Y}$ point on the Cu(511) surface. For the $\overline{Y}$ points, only the low energetic modes were identified in the calculations and no backfolding was found. No calculations were reported for the $\overline{\Gamma}$ point and, therefore, the existence and the character of a step edge mode was not found.

In a more recent study, Knipp[15] used the Green's function method to calculate the surface phonon dispersion curves along the step edge direction for nickel surfaces belonging to different symmetry classes of vicinal surfaces. He found three step localized surface modes close to the zone boundary. His values, when transformed to the copper surfaces studied here, are in good agreement with the frequencies of the longitudinal gap mode, the horizontal mode, and the Rayleigh mode at the $\overline{X}$ point of the Cu(211) surface. However, neither the step mode (E) observed in our experiments nor the edge mode near the $\overline{\Gamma}$ point were found in his calculations for any vicinal surface. He did, however, propose a similar mode for surfaces with kinked steps. For the fcc(511) surface, he found only a Rayleigh mode but no step phonon modes.

The surface phonon dispersion curves along the direction perpendicular to the step edges are sometimes discribed in terms of a backfolding of the terrace indexed surface modes.[13] Since the terrace planes progress into the crystal bulk and are tilted with respect to the macroscopic surface, the backfolding is linked with a projection of the wave vectors onto the macroscopic surface. This was first dicussed by Black and Lock[35] who carried out a folding of the "unit cell spectral density" in order to compare the terrace modes in an extended zone scheme with the phonon modes of the terrace indexed surfaces.

It is indeed quite surprising that the simple one force constant model used here to calculate surface phonon dispersion curves is sufficient to explain all the modes measured for both stepped copper surfaces. Moreover, even though no attempt was undertaken to fit the experimental dispersion curves, the calculated frequencies are also in remarkably good agreement. At the $\overline{Y}$ point, the agreement is 20%, while for the other symmetry points the agreement is better than 7%. This, of course, does not rule out the possibility of significant changes which might show up in a more sophisticated model. It does strongly suggest, however, that the character of phonon modes on stepped surfaces is predominantly determined by the special geometry of these surfaces and not by relaxation effects. On the other hand, the tendency of reconstruction and facetting of stepped copper surfaces induced by small amounts of adsorbates[36,5] does indicate their metastable equilibrium shape, which must be related to the presence of surface stress. Similar effects of stress were found for fcc(110) surfaces and their influence on the lattice dynamics has been reported previously for Ni(110) (Ref. 37) and Cu(110).[38] Moreover, the enhanced corrugation found from the diffraction patterns along the step edge direction of the Cu(211) surface when compared to the Cu(111) surface indicates a charge redistribution at the steps. Electronic relaxation at step edges, which is attributed to the Smoluchowski effect,[39] has been confirmed by several calculations,[40,41] which predict a reduced electron occupation of the edge atoms. The absence of diffraction for the corresponding direction of the Cu(511) surface indicates a smaller charge redistribution at the steps of this surface. This behavior is consistent with a step relaxation calculation by Jiang *et al.*,[34] which predicts a larger step atom inward relaxation for the fcc(211) than for the fcc(511) surface. We interpret the unexpected low transverse mode (T) energy along $\overline{\Gamma X}$ for Cu(211) compared with the theory as a consequence of step relaxation. Thus, even though there is considerable indirect evidence for both structural and electronic readjustments at step edges, the present

study has not been able to quantify their effect on the local force field at step edges.

Obviously the next step in the analysis of step phonons will be to calculate the intensities in the time-of-flight spectra. In this connection, it should be recalled that the anomalous intensities on the copper terrace surfaces uncovered serious shortcomings of the force constant models and eventually lead to the development of the pseudocharge model.[20] Such calculations are also of interest in order to better understand the scattering of molecules from stepped surfaces. Because of their lower vibrational frequencies, step edges should be more easily excited in collisions than terraces and thus steps provide sites with an enhanced trapping probability.[42]

Finally, we mention that in order to understand the dynamics of isolated defects, vicinal surfaces with larger terrace lengths need to be studied. Since the number of surface modes increases with the number of atoms within the unit cell, i.e., with increasing step distance, additional modes with bare step and terrace character are expected. Since each backfolded surface mode contributes a step mode at the $\bar{\Gamma}$ point and since the BZ length perpendicular to the steps becomes shorter for these surfaces, the energy of the step modes will have lower energies. The preparation of such surfaces is more difficult since the roughening temperature decreases with increasing terrace length.[2] One way to circumvent this problem is to use adsorbate induced step doubling. For example, we have been able to produce high quality surfaces with double steps from a Cu(211) surface by using an oxygen treatment.[36,43] The measurements of surface phonons on this surface will be reported elsewhere.

In summary, we have measured surface phonon dispersion curves over the entire Brillouin zone for regular stepped Cu(211) and Cu(511) surfaces. The existence and the character of step-localized modes beside the Rayleigh modes is demonstrated and well reproduced within a lattice dynamical analysis.

* Present address: Robert Bosch GmbH, D-70499 Stuttgart, FRG.

[1] G.A. Somorjai, *Chemistry in Two Dimensions: Surfaces* (Cornell University Press, Ithaca, NY, 1981).
[2] F. Fabre, D. Gorse, B. Salanon, and J. Lapujoulade, J. Phys. (Paris) **48**, 1017 (1987).
[3] E.H. Conrad, R.M. Aten, D.S. Kaufman, L.A. Allen, T. Engel, M. den Nijs, and E.K. Riedel, J. Chem. Phys. **84**, 1015 (1986); **85**, 4856(E) (1986).
[4] B.J. Hinch, A. Lock, H.H. Madden, J.P. Toennies, and G. Witte, Phys. Rev. B **42**, 1547 (1990).
[5] M. Sotto, Surf. Sci. **260**, 235 (1992).
[6] H.J. Ernst, F. Fabre, R. Folkerts, and J. Lapuloulade, Phys. Rev. Lett. **72**, 112 (1994).
[7] *Kinetics of Ordering and Growth at Surfaces*, edited by M.G. Lagally (Plenum Press, New York, 1990).
[8] J. Frohn, M. Giesen, M. Poensgen, J.F. Wolf, and H. Ibach, Phys. Rev. Lett. **67**, 3543 (1991). M. Giesen-Seibert, R. Jentjens, M. Poensgen, and H. Ibach, *ibid.* **71**, 3521 (1993).
[9] B.S. Swartzentruber, Y.W. Mo, R. Kariotis, M.G. Lagally, and M.B. Webb, Phys. Rev. Lett. **65**, 1913 (1990).
[10] E.D. Williams, Surf. Sci. **299/300**, 502 (1994).
[11] X.S. Wang, J.L. Goldberg, N.C. Bartelt, T.L. Einstein, and E.D. Williams, Phys. Rev. Lett. **65**, 2430 (1990).
[12] G. Benedek and J.P. Toennies, Surf. Sci. **299/300**, 587 (1994).
[13] G. Armand and P. Masri, Surf. Sci. **130**, 89 (1983).
[14] J.E. Black and P. Bopp, Surf. Sci. **140**, 275 (1984).
[15] P. Knipp, Phys. Rev. B **43**, 6908 (1991).
[16] H. Ibach and D. Bruchmann, Phys. Rev. Lett. **41**, 958 (1978).
[17] M. Wuttig, C. Oshima, T. Aizawa, R. Souda, S. Otani, and Y. Ishizawa, Surf. Sci. **193**, 180 (1988).
[18] J.P. Toennies, in *Surface Phonons*, edited by W. Kress and F. de Wette, Springer Series in Surface Science Vol. 21 (Springer-Verlag, Berlin, 1991).
[19] A. Lock, J.P. Toennies, and G. Witte, J. Electron Spectrosc. **54/55**, 309 (1990); *Proceedings of the Third International Conference on Phonon Physics and the Sixth International Conference on Condensed Matter, Heidelberg, 1989* (World Scientific, Singapore, 1990).
[20] C. Kaden, P. Ruggerone, J.P. Toennies, G. Zhang, and G. Benedek, Phys. Rev. B **46**, 13 509 (1991).
[21] G. Benedek, J. Ellis, N.S. Luo, A. Reichmuth, P. Ruggerone, and J.P. Toennies, Phys. Rev. B **48**, 4917 (1993).
[22] Since a stepped surface can be described as a convolution of a finite terrace with a regular step lattice, the resulting LEED diffraction pattern can be thought of as a product of the diffraction pattern from a terraces and the step lattice (Ref. 44). Therefore, Bragg (B) conditions exist whenever the diffraction maxima for terrace and steps coincide, while at anti-Bragg (AB) conditions, terrace diffraction minima coincide with step diffraction maxima. However, the observed LEED intensity is mainly determined by the terrace diffraction. In contrast, for HAS, vitually no diffraction results from the terraces since for helium atoms they are very smooth. Thus, the smooth He surface interaction potential of the terraces gives rise to multiple scattering and thus a modulation of the diffraction intensity with perpendicular momentum transfer.
[23] D. Gorse, B. Salanon, F. Fabre, A. Kara, J. Perreau, G. Armand, and J. Lapujoulade, Surf. Sci. **147**, 611 (1984).
[24] J. Braun, J.P. Toennies, and G. Witte (unpublished).
[25] G. Meyer, B. Neu, K.H. Rieder, U. Svenson, J.P. Toennies, and G. Witte (unpublished).
[26] In addition, an irregular stepped surface causes a phonon broadening due to lifetime limiting defect scattering.
[27] J.R. Manson, Comput. Phys. Commun. **80**, 145 (1994).
[28] R.E. Allen, G.P. Alldrege, and F.W. de Wette, Phys. Rev B **4**, 1648 (1971).
[29] R. Berndt, A. Lock, and Ch. Wöll, Surf. Sci. **276**, 213 (1992).
[30] We recall that our definition of the tangential α_i and radial β_i force constants (the index i refers to the ith nearest neighbor) is different from that given by Black *et al.* (Ref. 31), but can be converted to his definition: $\alpha_1 = \tilde{\alpha}_1 - \tilde{\alpha}_2$, $\alpha_2 = \tilde{\beta}_2$, $\beta_1 = \tilde{\alpha}_1 + \tilde{\alpha}_2$, and $\beta_2 = \tilde{\beta}_1$, where

the constants $\tilde{\alpha}_1$, $\tilde{\alpha}_2$, $\tilde{\beta}_1$, and $\tilde{\beta}_2$ are as described by Black *et al.*

[31] J.E. Black, D.A. Campbell, and R.F. Wallis, Surf. Sci. **115**, 161 (1981); J.E. Black, F.C. Shanes, and R.F. Wallis, *ibid.* **133**, 199 (1983).

[32] As shown in Fig. 6 also, the bulk bands are folded and surface resonances are smeared out over a large range of energies.

[33] A.M. Rodriguez, G. Bozzolo, and J. Ferrante, Surf. Sci. **289**, 100 (1993), and references therein.

[34] P. Jiang, F. Jona, and P.M. Marcus, Phys. Rev. B **35**, 7952 (1987).

[35] J.E. Black and A. Lock, Surf. Sci. **250**, 279 (1991).

[36] K.A. Thompson and C.S. Fadley, Surf. Sci. **146**, 281 (1984).

[37] S. Lehwald, F. Wolf, H. Ibach, B.M. Hall, and D.L. Mills, Surf. Sci. **192**, 131 (1987).

[38] P. Zeppenfeld, K. Kern, R. David, K. Kuhnke, and G. Comsa, Phys. Rev. B **38**, 12 329 (1988).

[39] R. Smoluchowski, Phys. Rev. **60**, 661 (1941).

[40] J. Tersoff and L.M. Falicov, Phys. Rev. B **24**, 754 (1981).

[41] J. Pancir, I. Haslingerova, and P. Nachtigall, Surf. Sci. **181**, 413 (1987).

[42] A.T. Yinnon, U. Minglegrin, and R.B. Gerber, J. Chem. Phys. **73**, 536 (1980).

[43] G. Witte, J. Braun, and J.P. Toennies (unpublished).

[44] M. Henzler, Appl. Phys. A **34**, 205 (1984).